ranging from 0.5 to 2.0 μs. The turn-on time of the pump was adjusted so that its leading edge corresponded smoothly with the leading edge of the signal pulse. The pump power was held constant at 1.5-watts peak for all cases. It will be noted that regardless of the pump pulse width the parametric coupling apparently occurs only during the initial turn-on time of the pump.

The character of the leading and trailing edges of this "spike gain" phenomenon can be seen more clearly in the expanded oscilloscope photograph shown in Fig. 2. Although the true response time of the magnetoelastic interaction process is probably masked by the relatively narrow-band (10 Mc/s) IF amplifier employed in the experimental arrangement, the observed transient suggests a very rapid initial buildup, followed by an exponential relaxation. Noise fluctuations on the tail of the decay inhibited any detailed observations of a ringing effect, which is suggested by the slight undershoot in the amplified pulses of Fig. 1.

It should also be pointed out that by using a suitably narrow signal pulse, the amplification can be made to take place for the entire pulse duration. As can be seen from Fig. 2, the width of the amplified portion of the signal pulse at the half-power points is about 0.5 μs. If superimposed on a signal pulse less than 1-μs wide, amplification effectively occurs over the entire pulse. Amplification of elastic waves by means of the "spike gain" phenomenon have resulted in electronic gains of 55 dB at room temperature, thus far.

One further experiment that was performed is illustrated by the series of oscilloscope photos shown in Fig. 3. In this case, the pump pulse width was held constant at 0.5 μs and the pump turn-on time, as represented by the upper trace in each photo, was smoothly varied across the width of the signal pulse. In Fig. 3(a) the leading edge of the pump pulse corresponds with the leading edge of the signal pulse. Figures 3(b), (c), and (d) select out successively later portions of the signal pulse including the trailing edge. Finally, in Fig. 3(e) only the elastic wave noise pulse[3] is visible in the absence of any interaction with a coherent signal.

This latter experiment demonstrates the feasibility of achieving a coherent variable delay that is electronically controllable through the turn-on time of the pump. By maintaining the input signal power just below the output level of detectability, the leading edge of the pump pulse might be used as a sensitive probe to raise the desired portion of the signal pulse out of the noise level. It is to be noted that the process described differs from the variable time delay of microwave pulse echoes reported by Damon and van de Vaart[4] for spin waves.

R. A. Sparks
E. L. Higgins
Amecom Div.
Litton Systems, Inc.
Silver Spring, Md.

[3] H. Matthews, "Elastic wave amplification in yttrium iron garnet at microwave frequencies," *Phys. Rev. Letters*, vol. 12, pp. 325–327, March 23, 1964.

[4] R. W. Damon, and H. van de Vaart, "Microwave pulse echoes with variable time delay by parametric pumping of traveling spin waves," *Appl. Phys. Letters*, vol. 6, pp. 194–196, May 15, 1965.

Linear Tuning of a Microwave Cavity

The usual tuning devices used with microwave cavities have pronounced nonlinear (frequency vs. probe position) characteristics because of their operation in nonuniform fields. The arrangment[1] described here encloses a small tuning probe with a dielectric sleeve of such shape as to improve the uniformity of the field around the probe and consequently the linearity of tuning over a useful range of operation.

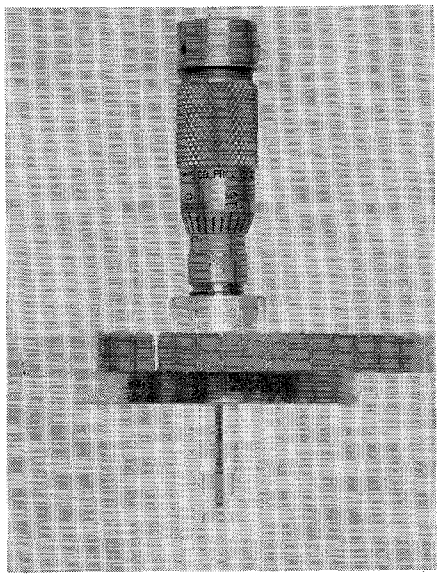

Fig. 1. Tuning probe enclosed in specially-shaped dielectric sleeve.

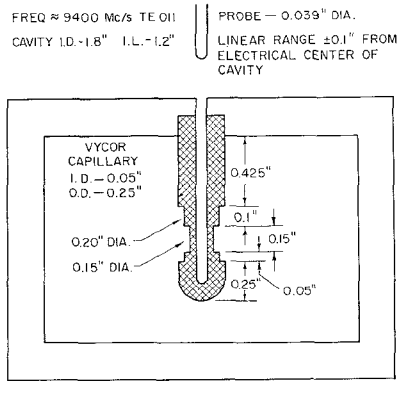

Fig. 2. Dimensional drawing of sleeve.

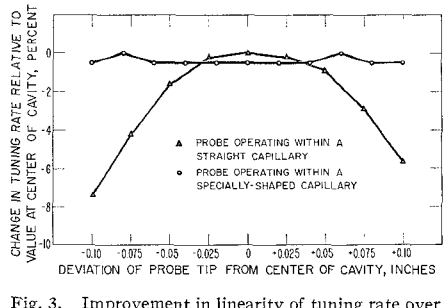

Fig. 3. Improvement in linearity of tuning rate over a range of ± 0.1 inch, expressed in per cent of tuning rate at center of cavity.

Manuscript received July 23, 1965.

[1] M. J. Vetter, "Movable resonant cavity tuning probe in dielectric sleeve having nonuniform outer surface," U. S. Patent 3 158 825, November 24, 1964.

General physical characteristics are shown in Figs. 1 and 2. The Vycor capillary has characteristics similar to fused quartz with a dielectric constant of approximately 3.8 and a very low dissipation factor.

Basically, the tuning probe is enclosed by more of the dielectric material in regions where the electric field would tend to be lower. This material concentrates the field in these regions and results in a uniform field over the desired range.

The choice of dimensions was arrived at empirically, and the effects are shown in Fig. 3.

A number of factors determine the optimum shape for the sleeve and effectiveness of the system. These include the dielectric constant of the sleeve, the diameter of the probe, the dimensions and configuration of the cavity, and the moninal field distribution in the region of the probe. The same concept could be used on cavities operating in other than the TE011 mode that was used here.

M. J. Vetter
Tropospheric Physics Section
Central Radio Propagation Lab.
National Bureau of Standards
Boulder, Colo.

Experimental Results in Groove Guide

This correspondence is concerned with the following developments in low-loss groove guide:

1) development of a transducer [1] from rectangular H_{10} mode to groove guide H_{11} (low-loss) mode,
2) experimental determination of transducer performance,
3) experimental verification of the dispersion relation and the attenuation constant obtained from the approximate theory developed by Ruddy [2]–[4] and Griemsmann [5] at the Polytechnic Institute of Brooklyn (PIB).

The mode transducer configuration is shown in Fig. 1. The inset shows a side view. The design is based, in some degree, on experience gained in the development of a mode transducer for low-loss H-guide [6] at PIB.

The transition is accomplished in two distinct steps. The first step is a transformation from rectangular waveguide to a special groove guide in which the plate separation b' in the extra-groove region is smaller than normal design value. This dimension is chosen such that the H_{10} parallel plate mode will be below cutoff for the highest frequency

Manuscript received April 23, 1965. The work reported here was sponsored by the Air Force Office of Scientific Research of the Office of Aerospace Research, under Contract AF 49(638)-1402.

of operation. This is done so that there will be minimal radiation loss via such a parallel plate mode in the region of coupling between closed rectangular waveguide and the open groove guide structure. The second step consists of increasing this dimension from the reduced value to the final value for the groove guide design. It should be noted that the plate separation in the groove region is equal to the wide dimension of rectangular waveguide. This was done solely as a matter of convenience.

Standard laboratory measurements of transducer insertion loss and input VSWR have been made, utilizing a sliding short in groove guide and substitution techniques, and the results are shown in Fig. 2. The physical length of the transducer, which was not optimized, accounts for approximately 0.2 dB of the insertion loss. It is felt, therefore, that a more efficient coupling design would reduce the coupling length (now approximately 20 wavelengths) by a factor of two and thereby reduce the insertion loss to a value below 0.2 dB over the entire frequency range. Thus, the transducer insertion loss would be equivalent to less than six inches of rectangular waveguide operating in the same frequency range.

It has been shown [1]–[5] that the dispersion relation for groove guide has the familiar form

$$\lambda_g = \frac{\lambda}{\sqrt{1 - \left(\frac{\lambda}{\lambda_c}\right)^2}}$$

where

$$\lambda_c = \frac{2\pi}{k_c};$$

$$k_c = \sqrt{\left(\frac{\pi}{b}\right)^2 + k_{yA}^2}$$

$$= \sqrt{\left(\frac{\pi}{b'}\right)^2 - |k_{yB}|^2}$$

where k_{yA} is the y-directed wavenumber in the groove region and $|k_{yB}|$ is the y-directed wavenumber in the outer region giving the decay rate in nepers per unit length (in y). Now k_{yA} and/or $|k_{yB}|$ are determined by the transverse procedure for a structure with specific dimensions. An experimental confirmation of the approximate theory was obtained for the case $a/b=3$ using a groove guide tunable reaction type cavity having $b=0.2800$ inch and $b'=0.270$ inch and a plate width of approximately 5 inches.

The cavity was excited by a capacitive iris in a transverse shorting plate at the input end and terminated in a shorting plate whose longitudinal position could be adjusted. The guide wavelength at any frequency was determined by measuring the distance between successive resonant positions of the tunable short. In Table I various values of guide wavelength are compared at a number of frequencies. The first two columns of guide wavelength permit a comparison of the measured values with those theoretically calculated. In the last column are predicted values of λ_g for a parallel plate mode if it were to exist rather than the bound groove guide mode. It is easily seen that the measured values of guide wavelength correspond to the predicted values for groove guide and at the same time differ greatly from the values predicted for parallel plate guide.

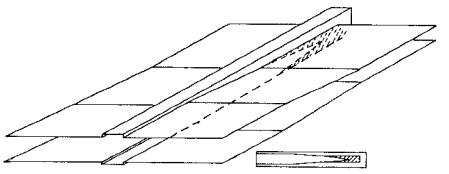

Fig. 1. Rectangular to groove guide transducer.

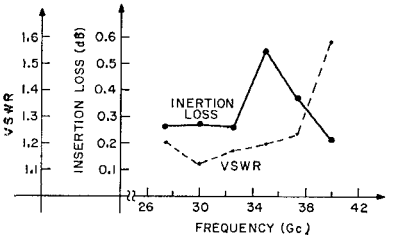

Fig. 2. Transducer performance.

TABLE I

f(Gc/s)	Measured λ_g(inches) G.G.	Calculated λ_g(inches) G.G.	Calculated λ_g(inches) P.P.
27.62	0 6803	0.6763	0.7055
28.82	0 6156	0.6117	0 6330
30.02	0.5622	0.5608	0.5771
31.96	0 5002	0.4974	0.5086
33.90	0 4492	0.4490	0.4572
35.86	0 4092	0.4102	0.4165
38.00	0.3774	0 3759	0.3807

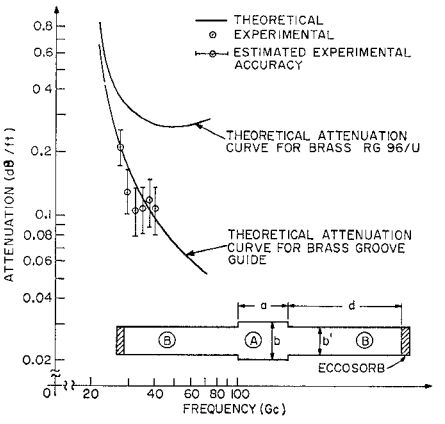

Fig. 3. Attenuation vs. frequency; groove guide no. 2 (machined brass); ($a=0.140$ inch, $b=0.280$ inch, $b'=0.250$ inch, $d=5.0$ inch).

The attenuation constant was measured using the groove guide sliding short and substitution. The groove guide under measurement was fabricated from machined brass and is shown in Fig. 3 with the experimental results.

JOHN M. RUDDY
Dept. of Electrophysics
Polytechnic Inst. of Brooklyn
Farmingdale, N. Y.

REFERENCES

[1] J. M. Ruddy, "The groove guide," Polytechnic Inst. of Brooklyn, N. Y., Progress Rept. 26 to Joint Services TAC, Rept. R-452.26-64, pp. 79–82, September 1964.
[2] ——, "Preliminary analysis of low loss groove guide," Polytechnic Inst. of Brooklyn, N. Y., Memo 78, Rept. PIBMRI-1127-63, February 1963.
[3] ——, "Grove guide," Polytechnic Inst. of Brooklyn, N. Y., Memo 89, Repts. PIBMRI-1177-63, July 1963.
[4] ——, "The groove guide," Polytechnic Inst. of Brooklyn, N. Y., Rept. PIBMRI-1240-64, October 1964.
[5] J. W. E. Griemsmann, "Groove guide," *1964 Proc. Symp. on Quasi-Optics*, vol. XIV, p. 365.
[6] L. Birenbaum and J. W. E. Griemsmann, "A low loss H-guide for millimeter wavelengths," *1959 Proc Symp. on Millimeter Waves*, vol. IX, p. 543.

Field Equations in Cylindrical Coordinates for Gyroelectric Media with Sources

For a gyroelectric medium characterized by a tensorial relative permittivity of the form

$$\bar{\bar{K}} = \begin{bmatrix} K_{11} & jK_{12} & 0 \\ -jK_{12} & K_{11} & 0 \\ 0 & 0 & K_{33} \end{bmatrix}$$

Maxwell's equations may be written as

$$\nabla \times \bar{H} = J_{ze}\bar{u}_z + \bar{J}_{te} + j\omega\epsilon_0 \bar{\bar{K}} \cdot \bar{E}$$

$$\nabla \times \bar{E} = J_{zm}\bar{u}_z + \bar{J}_{tm} - j\omega\mu_0 \bar{H}$$

where both electric and magnetic currents, designated by subscripts e and m, respectively, have been included. The currents have been separated into longitudinal and transverse components, designated by subscript z and t, respectively, with $\bar{u}_z$ representing a unit vector in the longitudinal direction. Throughout it is assumed that the fields and the currents have a time and z variation of the form

$$\exp(j\omega t - \gamma z).$$

Through the use of vector and tensor algebra, these two equations can be reduced to a set of wave equations which are in general coupled [1]. In matrix form they can be written as

$$\nabla_t^2 F + AF = J. \tag{1}$$

F and J are both two-dimensional vectors

$$F = \begin{bmatrix} E_z \\ H_z \end{bmatrix} \qquad J = \begin{bmatrix} J_1 \\ J_2 \end{bmatrix}.$$

A is a 2×2 matrix having elements a_{11}, a_{12}, a_{21}, and a_{22}; and ∇_t is the transverse part of the del operator

$$\nabla_t = \nabla - \frac{\partial}{\partial z}\bar{u}_z.$$

Defining

$$k_0^2 = \omega^2\mu_0\epsilon_0$$

$$k_1^2 = -k_0^2 K_{12}$$

and

$$k^2 = \gamma^2 + k_0^2 K_{11}$$

Manuscript received March 19, 1965; revised August 3, 1965.